

Original Research

Decoding Typical Flight States Based on Neural Signals from the Midbrain Motor Nuclei of Pigeons

Long Yang^{1,2,†}, Erteng Ma^{1,2,†}, Lifang Yang^{1,2}, Mengmeng Li^{1,2,*}, Zhigang Shang^{1,2,*}, Liaofeng Wang^{1,2}, Zuohao Ma^{1,2}, Jiajia Li^{1,2}¹School of Electrical and Information Engineering, Zhengzhou University, 450001 Zhengzhou, Henan, China²Henan Key Laboratory of Brain Science and Brain-Computer Interface Technology, 450001 Zhengzhou, Henan, China*Correspondence: limengmeng@zzu.edu.cn (Mengmeng Li); zhigang_shang@zzu.edu.cn (Zhigang Shang)

†These authors contributed equally.

Academic Editor: Gernot Riedel

Submitted: 27 September 2023 Revised: 14 November 2023 Accepted: 21 November 2023 Published: 3 April 2024

Abstract

Background: Exploring the neural encoding mechanism and decoding of motion state switching during flight can advance our knowledge of avian behavior control and contribute to the development of avian robots. However, limited acquisition equipment and neural signal quality have posed challenges, thus we understand little about the neural mechanisms of avian flight. **Methods:** We used chronically implanted micro-electrode arrays to record the local field potentials (LFPs) in the formation reticularis medialis mesencephali (FRM) of pigeons during various motion states in their natural outdoor flight. Subsequently, coherence-based functional connectivity networks under different bands were constructed and the topological features were extracted. Finally, we used a support vector machine model to decode different flight states. **Results:** Our findings indicate that the gamma band (80–150 Hz) in the FRM exhibits significant power for identifying different states in pigeons. Specifically, the avian brain transmitted flight related information more efficiently during the accelerated take-off or decelerated landing states, compared with the uniform flight and baseline states. Finally, we achieved a best average accuracy of 0.86 using the connectivity features in the 80–150 Hz band and 0.89 using the fused features for state decoding. **Conclusions:** Our results open up possibilities for further research into the neural mechanism of avian flight and contribute to the understanding of flight behavior control in birds.

Keywords: pigeon; flight state; FRM; LFP; functional connectivity

1. Introduction

The switching of external motion states exhibited by organisms, such as sudden acceleration and deceleration, often reflects changes in the internal state of the brain [1,2]. Effectively decoding the typical states has significant theoretical and practical implications for the understanding of internal movement intention encoding mechanisms, prosthetic control, and functional rehabilitation. It is also crucial for the development of future closed-loop brain computer interface technologies based on internal neural information decoding and external stimulation encoding. The decoding of neural information related to motor intentions or motion states in the brain has been extensively studied in various species including rats [3], primates [4,5], and birds [6,7].

Previous studies have indeed demonstrated that rhythmic information present in the brain can effectively represent different motor intentions or states [8,9]. For instance, Ahmadi *et al.* [10] successfully detected resting and force-generating time segments in the rat primary motor cortex using gamma (50–100 Hz) local field potentials (LFPs) during a key pressing task and accurately decoded the discrete rest/force states as well as continuous values of the force variable. Zhuang *et al.* [11] recorded LFPs using micro-electrode arrays in the primary motor cortex (M1) of non-

keys performing reaching and grasping tasks. Their mutual information and decoding analysis revealed that higher frequency bands (e.g., 100–200 and 200–400 Hz) carried the most information about the examined kinematics, suggesting the utility of LFPs, especially high-frequency bands, for controlling reach and grasp movements. Bundy *et al.* [12] used a hierarchical partial-least squares (PLS) regression model to predict hand speed, velocity, and position based on electrocorticography (ECoG) signals recorded from epileptic patients performing a 3D center-out reaching task. Their findings highlighted the importance of beta band power changes for classifying movement and rest, as well as local motor potential and high gamma band power changes for predicting kinematic parameters. Although a series of evidence shows that the movement state of organisms can be decoded by recording neural activities in the brain and extracting relevant rhythm features [13], most studies have been restricted by the signal acquisition equipment and the ability to examine only specific scenarios within the laboratory, leading to a large disparity between research and practical application.

Compared with rodents and primates, the pigeon possesses exceptional flying capabilities and is not constrained by ground environments [14], making it an ideal animal



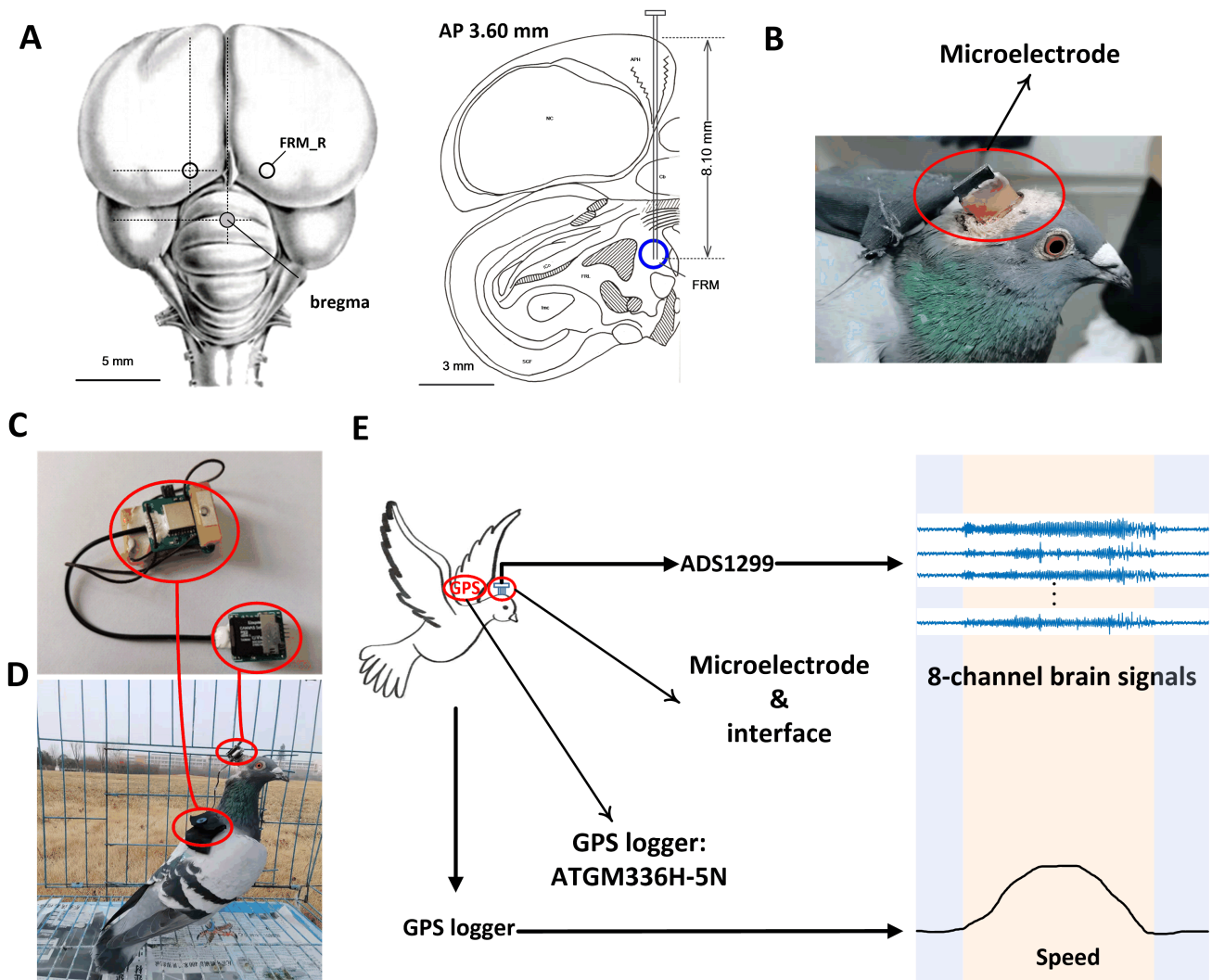


Fig. 1. Electrode implantation and data acquisition. (A) Location of microelectrode implantation. (B) Pigeon implanted with a microelectrode array. (C) Wearable data recording device. (D) Pigeon wearing the data recording device. (E) Diagram of data recording during free flight, in which the 8-channel LFP signals and the GPS data were recorded. AP, anteroposterior; FRM, formation reticularis medialis mesencephali; GPS, global positioning system; LFP, local field potential.

model for studying natural motion states, especially flight states. Notably, studies have demonstrated that micro-current stimulation in the formation reticularis medialis mesencephali area (FRM) of the pigeon brain can induce turning actions [15]. During flight, the direction of flight can be regulated by applying electrical stimulation to this specific brain area [16]. However, it is important to consider the animal's autonomous movement intentions to avoid potential negative effects on regulation efficacy or physical fitness when external stimulation instructions do not align with the animal's movement intentions. In this regard, it is crucial to investigate and understand the neural decoding of autonomous movement intentions during flight. However, it is worth noting that despite these promising findings, most of the existing research on decoding the different motion states of pigeons is restricted by the equipment used for signal acquisition and experiments

can only be conducted in specific laboratory settings [17], allowing only limited exploration of flight processes.

Thanks to the advancements of integrated circuit technology and microcontroller technology, signal recorders suitable for small animals in natural conditions have been developed for use in related research. In 2019, Massot *et al.* [18] introduced a new tool called ONEIROS, which enabled sleep research in small, freely moving animals. They demonstrated the practicality of the device by successfully recording a pigeon in an 8 m^3 aviary with a social context in the logger configuration. In 2020, we designed a wearable signal recording system to synchronously record the neural activities, attitude data, and position information of birds during flight [19]. Our experimental results showed that the system could meet the needs of robust data recording without impeding the birds' normal flight. These technological advancements not only facilitate the study of neural

information decoding in birds during flight but also provide a solid foundation for further research in this area.

We therefore used pigeons, and the FRM associated with their flight as the target region, to investigate the autonomous flight intentions in the bird brain during natural flight in this study. We used our wearable signal recording system to simultaneously record the neural signals in the FRM and the posture information of three pigeons during their free flying. Four typical flight states, including baseline, accelerated take-off, uniform flight, and decelerated landing, were defined via analysis of global positioning system (GPS) data. Using coherence analysis, brain function connectivity networks were constructed based on the multi-channel LFP signals corresponding to the various states. Based on the topological characteristic analysis results of the functional connectivity networks, distinct features in the gamma frequency band (80–150 Hz) were extracted for decoding the four typical flight states and the results were compared with the other bands. To the best of our knowledge, this is the first study focused on the neural information decoding of different outdoor flight states of pigeons, providing a valuable reference for further research on the neural mechanism of avian flight, navigation, and behavior control in birds.

2. Materials and Methods

2.1 Subjects and Electrode Implantation

In this study, a total of six adult homing pigeons (*Columba livia*, 450–500 g, unknown sex) obtained from a local supplier (Gongchuang Pigeon Co., Zhengzhou, Henan, China) were used. All pigeons were housed in a loft, provided with regular feeding by professionals and free drinking water in their normal living conditions. The pigeons' diet was restricted during flight tasks until completion of the experiment. All experimental procedures adhered to the guidelines outlined in the Animals Act, 2006 (China), and aimed to ensure the ethical care and use of laboratory animals. The study protocol was approved by the Life Science Ethical Review Committee of Zhengzhou University (No. SYXK 2019-0002).

Once it was established that the pigeons were capable of reliably completing the flight task, we implanted microelectrode arrays into the FRM of pigeons, in which eight individually insulated tungsten microwires (California Fine Wire, Grover Beach, CA, USA) with a 35- μm inner diameter and 150- μm spacing between the wires (Kedou Brain Computer Technology, Suzhou, Jiangsu, China) were used. The surgical procedure followed a similar protocol as described in our previous study [20]. Initially, pigeons were anesthetized using a 3% sodium pentobarbital solution (at a dose of 0.12 mL/100 g body weight, $\text{C}_{11}\text{H}_{17}\text{N}_2\text{NaO}_3$, Shanghai Toscience Biotechnology Co., Ltd, Shanghai, China) and securely placed in a stereotaxic apparatus. Next, the location of the FRM was determined using a stereotaxic map of the pigeon brain [21] as

a guide. Finally, the 8-channel microelectrode array (Customized version, Kedou Co., Suzhou, Jiangsu, China) was implanted into the target point with the following coordinates: anteroposterior (AP) 3.60 mm, mediolateral (ML) 1.20 mm, and dorsoventral (DV) 8.10 mm. The specific position of the electrode implantation and the pigeon after the implantation are shown in Fig. 1A,B, respectively.

2.2 Apparatus and Experimental Task

To simultaneously record the flight state related GPS data of pigeons and their neural signals in the FRM, a wearable data recording device was developed, which was described extensively in our previous publication [19] and is shown in Fig. 1C. The self-made device (Henan Key Laboratory of Brain Science and Brain-Computer Interface Technology, Zhengzhou, Henan, China) weighed 13.6 g and consisted of a GPS module (ATGM336H-5N with sampling range of 1–10 Hz, positional accuracy <2.5 m circular error probable) and a neural signal acquisition module (8-channel ADS1299 from Texas Instruments (ADS1299IPAGR, TI Co., Dallas, TX, USA) with sampling rate range of 0.25–16 KHz, magnification 1–24, and conversion accuracy 0.1 $\mu\text{V/bit}$). It should be noted that the GPS data were used for the definition of the typical flight states of pigeons.

Before recording, the pigeons were trained to perform in the study by wearing backpacks to increase their capacity for bearing weight for 2 weeks. The study mainly consisted of a pre-experiment and a formal experiment. In the first week, the pigeons were loaded with 20-g weight during both walking and flying to adapt to the burden of the device. In the second week, the pigeons were released daily on short-distance (2 km) flights away from the loft. After the pre-experiment, the pigeons wore our data recording device as shown in Fig. 1D. During the whole flight process, including baseline, accelerated take-off, uniform flight, and decelerated landing, 8-channel neural signals and GPS data were recorded synchronously as depicted in Fig. 1E.

2.3 Data Acquisition and Analysis

We performed GPS and LFP data acquisition during the flight of pigeons from the release site to the home loft as shown in Fig. 2. The sampling rate of GPS data is 10 Hz and that of the LFP signal is 1000 Hz. The GPS data provides essential information regarding the pigeon's latitude and longitude coordinates during free-flying, as well as velocity data. The acceleration of the pigeon during flight can be further calculated based on the velocity data as follows:

$$a = \frac{dv}{dt} \quad (1)$$

When pigeons are flying outdoors, the neural signals can be prone to interference from baseline drift and noise generated by their flapping wings. To address these chal-

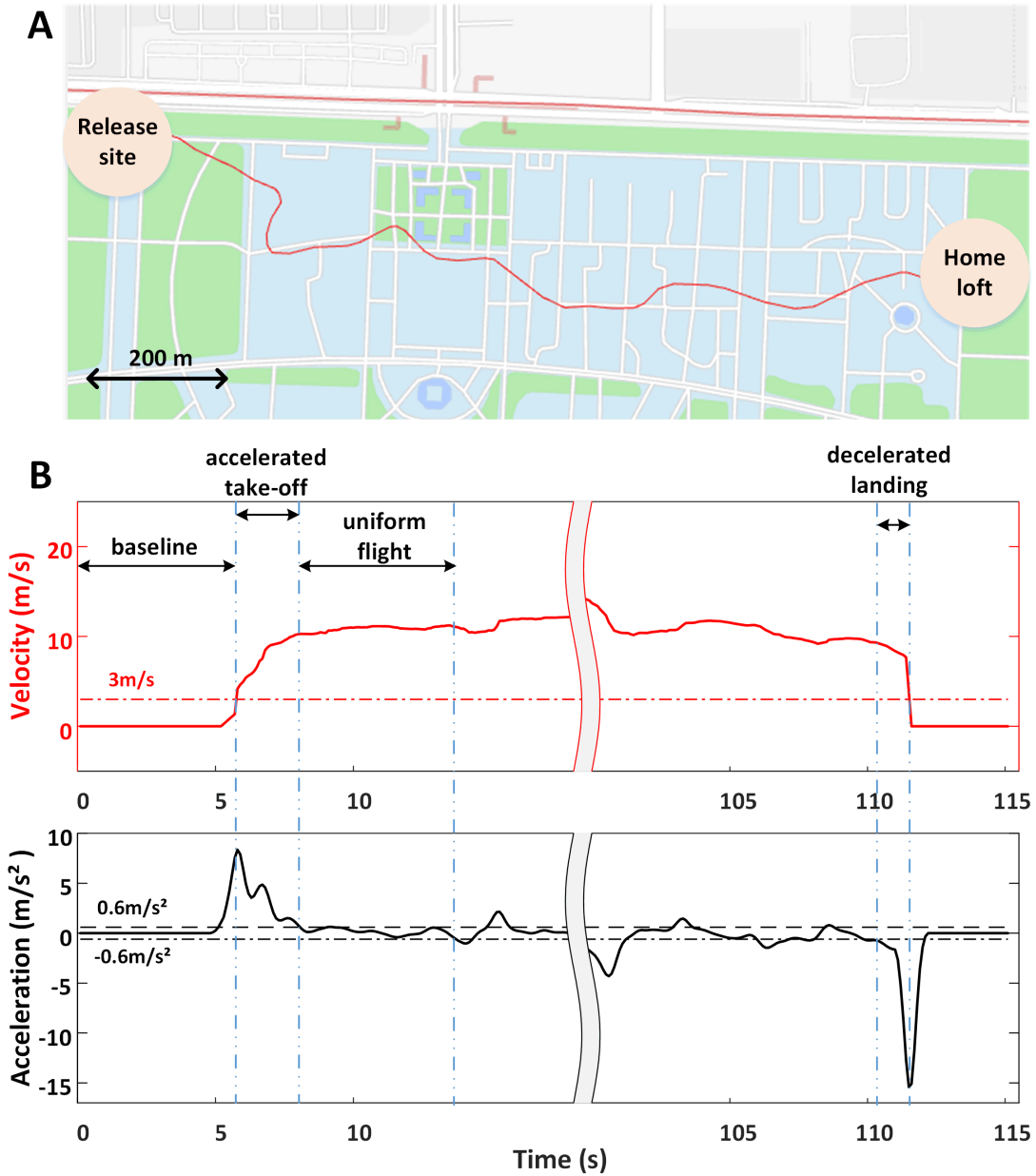


Fig. 2. Recorded GPS track and definition of typical states. (A) The track is displayed on the map, where the red line indicates the actual flight route from the release site to the home loft. (B) The velocity and acceleration curve calculated after pre-processing the GPS data, in which the solid red line represents the change of speed, and the solid black line represents the corresponding change of acceleration, marking four typical motion states based on the velocity and acceleration curves.

lenges, it is important to eliminate the trend terms from the neural signals and account for the non-stationary nature of the signal. Firstly, to accomplish baseline drift, discrete wavelet transform (DWT) was employed. The DWT is defined as follows:

$$W_{\varphi}f(j, k) = \int s(t)\varphi_{j,k}^*(t)dt \quad (2)$$

where $s(t)$ is the temporal neural signal, $\varphi_{j,k}(t) = 2^{-\frac{j}{2}}\varphi(2^{-j}t - k)$ is the base function, i is the frequency res-

olution, and j is the time shift. In this study, we performed a 10-layer discrete wavelet decomposition to process the original signal using the 'sym8' wavelet packet. We then reconstructed the 2–250 Hz sub-band signals to obtain the targeted LFPs without the baseline drift.

To address the issue of flapping noise in the neural signals, the primary method used is priori variational modal decomposition (VMD). This technique aims to extract intrinsic mode functions or modes of oscillation from the signal without relying on fixed functions for analysis. This makes it particularly effective for processing non-smooth

and non-linear neural signals. The fundamental concept behind VMD is to construct and solve variational problems [22]. Previous studies have indicated that pigeons exhibit vibrations in the frequency range of approximately 3–10 Hz during flight [23,24]. According to this prior knowledge, modal components within this frequency range are discarded. The remaining modal components are then reconstructed to obtain the processed LFP signal. In the current study, our multi-channel LFPs were filtered using a zero-phase bandpass filter to obtain signals in the following four frequency bands: β (12–30 Hz), γ_1 (30–80 Hz), γ_2 (80–150 Hz), γ_3 (150–250 Hz).

2.4 Typical Flight States Definition

In this study, we focused on four typical flight states of pigeons: baseline, accelerated take-off, uniform flight, and decelerated landing. Previous studies have commonly used GPS speeds greater than 5 or 10 km/h to identify pigeons in flight [25,26]. However, in this study, we considered the actual movement of the pigeons during flight and the accuracy of the sensors to define the above typical states. For small fluctuations in speed within a certain range (± 0.3 m/s), we considered the pigeon to be flying at a constant speed. For take-off and landing states, we define them using flight speed and acceleration considering their observed significant changes. The state “uniform flight” refers to a state of constant speed flight. This approach acknowledges the agility and flexibility of pigeons in controlling their flight speed. Based on these considerations, the following principles were used to define the four motion states:

(1) Baseline: This state represents a continuous process in which the pigeon’s speed is less than 3 m/s. It typically corresponds to the pigeon being at rest on the ground.

(2) Accelerated take-off: This state represents a continuous process in which the pigeon’s speed is greater than 3 m/s, and the acceleration is greater than 0.6 m/s^2 . It signifies the pigeon’s initial acceleration during take-off.

(3) Uniform flight: This state represents a continuous process in which the pigeon’s speed is greater than 3 m/s, and the absolute value of the acceleration is less than 0.6 m/s^2 . It indicates the pigeon’s consistent flight at a relatively constant speed.

(4) Decelerated landing: This state represents a continuous process in which the pigeon’s speed is greater than 3 m/s, and the acceleration is less than -0.6 m/s^2 . It corresponds to the pigeon’s gradual deceleration during landing.

2.5 Functional Connectivity Analysis

We then explored the connectivity between multiple channel LFPs in the FRM to find effective features on the scale of local network connections for decoding the four states. This is accomplished by generating a connection matrix that represents the relationship between different channels or brain regions. Subsequently, the topological properties of the brain function connectivity network are analyzed

using principles from graph theory. In this study, the connectivity network was established by quantifying the coherence between channels. The coherence coefficient is calculated as follows:

$$C_{xy}^2(f) = \frac{|S_{xy}(f)|^2}{S_{xx}(f) * S_{yy}(f)} \quad (3)$$

where S_{xy} is the cross-power spectral density of signals $x(t)$ and $y(t)$, and S_{xx} and S_{yy} are their self-power spectral densities, respectively.

To measure the topological characteristics of the connectivity network, the clustering coefficient (Cc), global efficiency (Ge), and average path length (Apl) were calculated specifically. The clustering coefficient quantifies the tendency for neighboring channels to form interconnected clusters [27]. It provides a measure to evaluate the level of network integration and can be defined as follows:

$$C_c = \frac{1}{N} \sum_{i=1}^N C_i = \frac{1}{N} \sum_{i=1}^N \frac{2E_i}{k_i(k_i - 1)} \quad (4)$$

where N represents the total number of nodes in the network, k_i is the node degree (number of connections) of node i , and E_i denotes the total number of triangles formed by the neighbors of node i . A larger clustering coefficient suggests that nearby neurons have a higher likelihood of being connected, creating tightly-knit groups within the network.

The global efficiency provides insights into the efficiency of information flow across the network and is defined as the average value of the path length between two nodes in the network as follows:

$$G_e = \frac{2}{N * (N - 1)} \sum_{i,j \in V, i \neq j} \frac{1}{d_{ij}} \quad (5)$$

where N represents the total number of nodes in the network and d_{ij} represents the path length between node i and node j . The higher the global efficiency, the more efficiently the information is transferred between different channels.

The average path length represents the average number of edges required to traverse between any two channels in the network. It provides a measure of the global efficiency of information transmission or integration across the entire network and can be defined as:

$$L = \frac{2}{N(N - 1)} \sum_{i,j \in V, i \neq j} d_{ij} \quad (6)$$

where d_{ij} represents the path length between node i and node j . A smaller average path length indicates that there are shorter and more direct pathways between different channels, facilitating efficient information exchange.

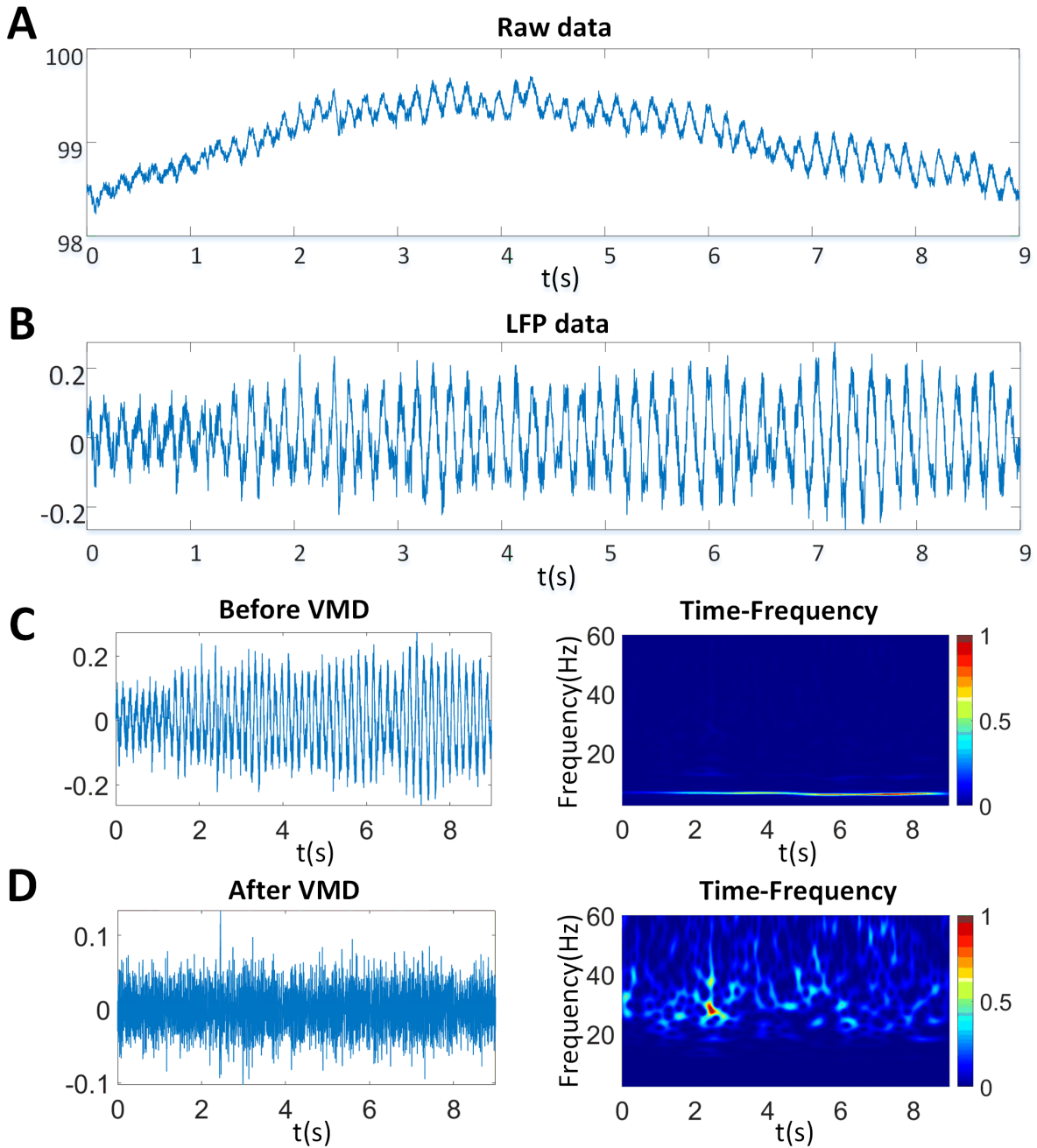


Fig. 3. Neural signal pre-processing. (A) Raw neural signals. (B) LFP signal processed to remove baseline drift by wavelet technology. (C) LFP signals before VMD in time and time-frequency domain. (D) The LFP signals after VMD in time and time-frequency domain. VMD, variational modal decomposition.

2.6 Decoding and Statistical Analysis

We analyzed the differences in connectivity characteristics of the four typical states and extracted effective features for the decoding analysis. Support vector machine (SVM) models can better solve the problem of small sample classification and have been successfully applied in many fields [28]. Thus, an SVM was used in this study for typical flight state decoding and the performance was assessed through ten-fold cross-validation.

Our results are given in the form of mean \pm standard deviation (SD) unless otherwise specified. The statistical differences between different groups or conditions were evaluated using the Kruskal-Wallis test, which is a non-parametric test method. The significance level for determining statistical significance was set at 5% and p -values were considered statistically significant as follows: * $p < 0.05$, ** $p < 0.01$, *** $p < 0.001$.

Table 1. Experimental data of pigeons.

Pigeon	No. of channels	No. of sessions	No. of signal segments			
			Baseline	Accelerated take-off	Uniform flight	Decelerated landing
P02	8	12	86	66	94	83
P03	8	13	116	92	97	89
P06	8	15	106	108	99	90

3. Results

3.1 Data Pre-Processing Results

We effectively collected the data of three pigeons (P02, P03, and P06), while three other animals (P01, P04, and P05) dropped out of the study due to electrode implantation failure or poor signal quality. The pigeons were released from a location about 2 km away from the loft, and one whole flight process recorded by GPS data of P02 is shown in Fig. 2A. The speed and acceleration information of pigeons was calculated based on the GPS data to better characterize their specific states. Four typical motion states including baseline, accelerated take-off, uniform flight, and decelerated landing were then defined according to the above calculations, which are shown in Fig. 2B.

For the recorded neural signals, we have shown a pre-processing example of 5 s of data during the study of P02. Fig. 3A shows the raw signal obtained from one of the acquired channels, in which there is a baseline drift. We then applied the DWT to remove the drift, and the result is shown in Fig. 3B. Fig. 3C shows the time-frequency analysis results of the LFPs, and there is a noticeable wing coupling component with a frequency range of approximately 5–10 Hz. Next, we employed VMD to mitigate the wing-flapping noise; Fig. 3D displays the signal and time-frequency analysis results after VMD.

Each pigeon underwent a different number of sessions, with 12, 13, and 15 sessions respectively in the current study (each session represents one flight experiment). According to the definition of the typical states, we obtained the corresponding neural signals and divided them into segments of 500 ms windows. Table 1 shows the experimental data for three pigeons.

3.2 Power Spectrum and Functional Connectivity Analysis Results

We first compared the results of the power spectrum analysis at different frequency bands in four typical states and the results are shown in Fig. 4A. We observed distinct power spectrum differences among these four typical states, with the most notable discrepancies occurring in the γ_2 band, followed by the γ_1 band, β band, and γ_3 band. Thus, we constructed a distribution diagram for the functional network topology characteristics in the γ_2 band of P02 shown in Fig. 4B, in which the subgraph along the diagonal represents the probability density of each feature and the other subgraphs represent the feature distribution between char-

acteristics. The four typical states show distinguishable density distributions from each other, especially for the clustering coefficient and the global efficiency. Specifically, the mean value of the characteristic probability density is highest for the accelerated take-off state and lowest for the baseline state across all three characteristics. Furthermore, from the visualization results that consider the distribution of two-dimensional topological characteristics, we identified clear separability among multiple states. Specifically, the baseline state can be completely distinguished from the other three states in all cases. Between the remaining three states, there are relatively clear classification boundaries observed between the accelerated take-off and uniform flight states, and decelerated landing, while the distributions of the decelerated landing states appear to be partially overlapping between them.

We then calculated the clustering coefficient, global efficiency, and average path length of the functional networks for the four states of three experimental pigeons using graph theory. The statistical analysis results of the clustering coefficient for the bands are shown in Fig. 4C. For the inter-state comparisons, it is apparent that the clustering coefficients for all three typical flight states of the three pigeons are significantly higher (Kruskal-Wallis test, $p < 0.001$) than that during the baseline state in the vast majority of cases (except for the baseline versus the uniform flight and decelerated landing states in the β band; Kruskal-Wallis test, $p > 0.05$). This implies that the brain exhibits a higher level of network integration for effective information transmission during flying. Furthermore, the analysis reveals that the functional connectivity is tighter during state-shifting of flight including the accelerated take-off and decelerated landing states compared with uniform flight, especially for all pigeons in the γ_2 band (Kruskal-Wallis test, $p < 0.001$). This suggests a frequency-specific neural mechanism to encode the transitional phases during flight. For the inter-band comparisons, the characteristics of the γ_2 band demonstrate significant differences across all four states and for all three pigeons (Kruskal-Wallis test, $p < 0.05$). This suggests that the γ_2 band may contribute to the distinct neural patterns for shifting among different states. Finally, it should be noted that we observed identical or similar results in the inter-state statistical analysis of the other two topological characteristics.

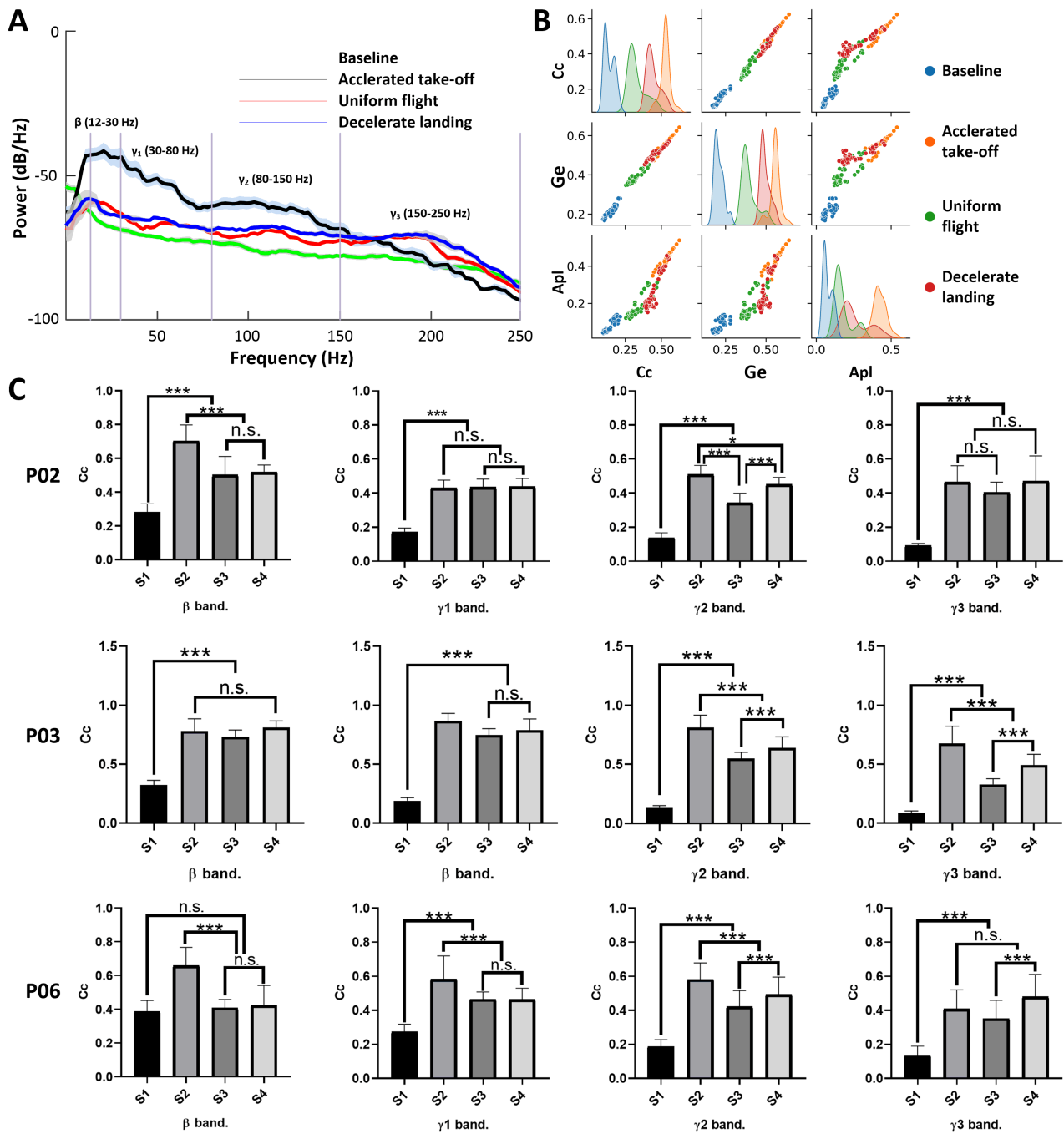


Fig. 4. Power spectrum and functional connectivity analysis results. (A) Power spectrum analysis of the LFPs during four typical states. (B) Functional network characteristic distributions of the γ_2 band LFPs for P02 during four states (Cc, clustering coefficient; Ge, global efficiency; Apl, average path length). (C) Statistical analysis results of clustering coefficients for three pigeons during four different states (s1, baseline; s2, accelerated take-off; s3, uniform flight; s4, decelerated landing; * $p < 0.05$, *** $p < 0.001$; n.s., no significance).

3.3 Decoding Results

The functional connectivity characteristics from the FRM showed variability across four typical states. We therefore sought to ascertain with what accuracy could the pigeon's current states during flight be determined based on

the functional connectivity features. To answer this question, a multi-classified SVM was used to decode the pigeon's states and the analysis results are shown in Fig. 5 (detailed results are shown in **Supplementary Table 1**). The typical flight state decoding accuracy of three pigeons is shown in Fig. 5A. The results indicate that the accuracy

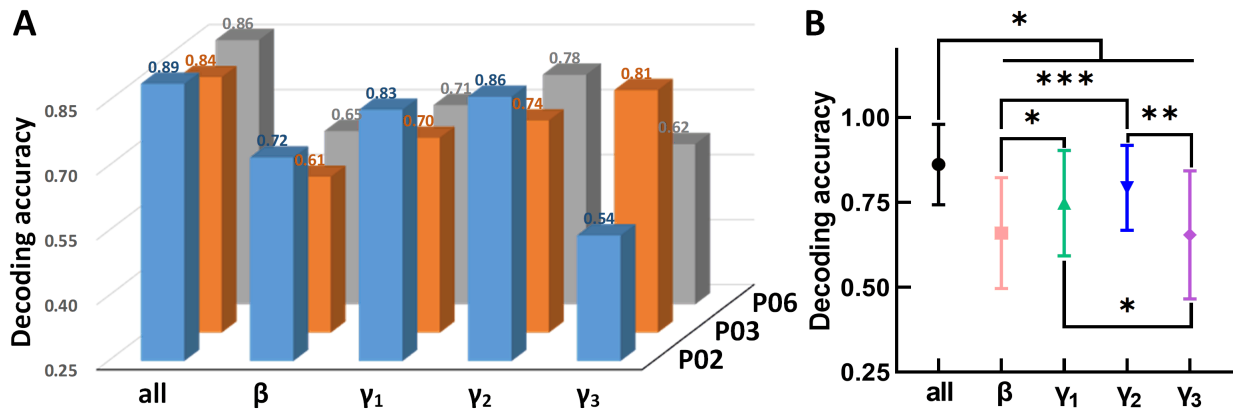


Fig. 5. Decoding analysis results using functional connectivity features. (A) Decoding accuracy of typical flight states of three pigeons. (B) Decoding results across all pigeons (* $p < 0.05$, ** $p < 0.01$, *** $p < 0.001$).

varies across the four different frequency bands. The best average decoding results for P02 and P06 are achieved in the γ_2 band (0.86 and 0.78), while the highest accuracy for P03 is observed in the γ_3 band (0.81). When considering the overall decoding accuracy using the fused feature set including features in all four bands, P02, P03, and P06 achieve average accuracies of 0.89, 0.84, and 0.86, respectively. This suggests that flight related information of the pigeon could be encoded via specific bands in the FRM and could be decoded by the corresponding neural patterns in these bands.

The statistical decoding results across all three pigeons are shown in Fig. 5B. We observed the best decoding performance using all features in the four bands across the three pigeons, which was significantly higher than those using the features in other single frequency bands (0.86 ± 0.12 versus 0.66 ± 0.16 , 0.75 ± 0.16 , 0.79 ± 0.13 , 0.65 ± 0.19 ; Kruskal-Wallis test, $p < 0.05$). For the performance using the features in the γ_2 band, the average decoding accuracy for the states was significantly higher than those using the features in the β band (0.79 ± 0.13 versus 0.66 ± 0.16 ; Kruskal-Wallis test, $p < 0.001$) and the γ_3 band (0.79 ± 0.13 versus 0.65 ± 0.19 ; Kruskal-Wallis test, $p < 0.01$). Similarly, the average accuracy using the features in the γ_1 band was also significantly higher than those in the β band (0.75 ± 0.16 versus 0.66 ± 0.16 ; Kruskal-Wallis test, $p < 0.05$) and the γ_3 band (0.75 ± 0.16 versus 0.65 ± 0.19 ; Kruskal-Wallis test, $p < 0.05$). There was no significant difference between the performance of the γ_2 band and γ_1 band (0.79 ± 0.13 versus 0.75 ± 0.16 ; Kruskal-Wallis test, $p > 0.05$). These findings demonstrate that the γ_2 band and γ_1 band consistently showed relatively high state decoding accuracy across the three pigeons. This may suggest that these frequency bands contain the most relevant encoding information related to the pigeon's flight. In addition, we also compared the typical flight states decoding results of the three pigeons using LFP power features (detailed results

are shown in **Supplementary Table 2**). The best decoding performance using all features and the superior results in the γ_2 band were also observed.

4. Discussion

This study explored the neural activity analysis and state decoding of pigeons during flying under natural outdoor conditions. The results revealed that the FRM of pigeons encoded the flight related information, particularly the state switching related information. We found that high-frequency functional connectivity in the FRM, especially in the gamma band (80–150 Hz), better characterized the flight state of the pigeon compared with the other bands. The decoding analysis results also provide insights into the neural processes underlying different states during pigeons' flight. It should be noted that previous research has linked high-frequency rhythm activity to multiple functions including motor, attention, and decision-making [29–31]. Our findings align with previous studies in other animal species, suggesting the relevance of the gamma band in locomotion [10,11].

Despite the findings, there are limitations in the study, including but not limited to verifying the validity of the data, behavioural control based on flight decoding, and further optimization of site localization by staining slices. First, our study contains data for analysis from only three pigeons, constrained by the difficulty in constructing avian flight experimental paradigms in large-scale natural environments and the difficulty in collecting and denoising neural signals under free-flying conditions. In addition, incomplete experimental data problems as mentioned caused by difficult electrode surgical implantation and postoperative recovery, as well as accidental loss or death of pigeons, also pose challenges for us to expand the sample and data size. Hence, more pigeons and data are needed to further improve the accuracy and robustness of our results. Furthermore, it is known that the direction of flight can be regulated by ap-

plying electrical stimulation to this specific brain area during flight [15,16,32]. Applying different stimulation parameters to pigeons can also induce varying turning angles [33]. By stimulating individuals, researchers can study flapping flight and collective behaviour in pigeon flocks [34]. Further study focused on the behavioural control of birds based on flight state recording and decoding should therefore be carried out. Additionally, further detailed exploration of the structural characteristics of the FRM with the help of stained slices, together with examination of the specific functions of the left and right hemispheres [35,36] of the FRM and their relationship with autonomous steering intention, could enhance the understanding of motion state decoding during bird flight.

Regarding the remaining issues and areas for further study, it is indeed important to consider factors beyond speed changes and incorporate different steering information during flight [37]. In terms of brain regions and physiological measurements, it is worth noting that other brain regions may provide targets for future movement intention decoding. For example, the activity in the opticus principalis thalami (OPT) has been previously linked to computing the distance-to-collision of approaching surfaces in pigeons [35]. Furthermore, considering correlations between other kinds of recordings apart from GPS tracking measurements alongside oscillatory recordings could provide valuable complementary information. In addition, there are also potential limitations in the experimental period regarding the individual characteristics of the pigeon and environmental factors, the data pre-processing process of artifact removal, and the decoding process using the SVM. We aim to eliminate these negative influencing factors to better optimize our future studies.

5. Conclusions

Overall, our results contribute to filling a knowledge gap and provide valuable support for further studies on avian motion state decoding and flight behaviour control, supporting closed-loop brain-computer interfaces for birds that consider both internal neural encoding and external behavioural decoding. In addition, our results show that our recording device can provide valuable insights for long-distance flight and navigation related research.

Availability of Data and Materials

The datasets used and/or analyzed during the current study are available from the corresponding author upon reasonable request.

Author Contributions

LY, ML, and ZS designed the study. LY and EM performed the research. LY and LW designed and assembled the device. LY, EM, LFY, and ZM conducted experiments. LY, LFY, and ML analyzed the data. LFY and JL per-

formed the validation and visualization. LY and ML performed the investigation. LY and ML prepared the original draft. ML and ZS reviewed and edited the draft. All authors have read and agreed to the published version of the manuscript. All authors contributed to editorial changes in the manuscript. All authors read and approved the final manuscript. All authors have participated sufficiently in the work and agreed to be accountable for all aspects of the work.

Ethics Approval and Consent to Participate

The study was conducted in accordance with the Declaration of Helsinki, and the protocol was approved by the Life Science Ethical Review Committee of Zhengzhou University (No. SYXK 2019-0002).

Acknowledgment

Not applicable.

Funding

This work was supported by the National Postdoctoral Researcher Program (GZC20232447), the National Natural Science Foundation of China (62301496), and the Key Scientific and Technological Projects of Henan Province (232102210098, 222102310223).

Conflict of Interest

The authors declare no conflict of interest.

Supplementary Material

Supplementary material associated with this article can be found, in the online version, at <https://doi.org/10.31083/j.jin2304072>.

References

- [1] Yoshino K, Oka N, Yamamoto K, Takahashi H, Kato T. Correlation of prefrontal cortical activation with changing vehicle speeds in actual driving: a vector-based functional near-infrared spectroscopy study. *Frontiers in Human Neuroscience*. 2013; 7: 895.
- [2] Mierau A, Klimesch W, Lefebvre J. State-dependent alpha peak frequency shifts: Experimental evidence, potential mechanisms and functional implications. *Neuroscience*. 2017; 360: 146–154.
- [3] Heydari Beni N, Foodeh R, Shalchyan V, Daliri MR. Force decoding using local field potentials in primary motor cortex: PLS or Kalman filter regression? *Physical and Engineering Sciences in Medicine*. 2020; 43: 175–186.
- [4] Pesaran B, Pezaris JS, Sahani M, Mitra PP, Andersen RA. Temporal structure in neuronal activity during working memory in macaque parietal cortex. *Nature Neuroscience*. 2002; 5: 805–811.
- [5] Scherberger H, Jarvis MR, Andersen RA. Cortical local field potential encodes movement intentions in the posterior parietal cortex. *Neuron*. 2005; 46: 347–354.
- [6] Liu X, Zhao K, Wang D, Ping Y, Wan H. Goal-directed behavior elevates gamma oscillations in nidopallium caudolaterale of pigeon. *Brain Research Bulletin*. 2018; 137: 10–16.

- [7] Rinnert P, Nieder A. Neural Code of Motor Planning and Execution during Goal-Directed Movements in Crows. *The Journal of Neuroscience*. 2021; 41: 4060–4072.
- [8] Engel AK, Fries P. Beta-band oscillations—signalling the status quo? *Current Opinion in Neurobiology*. 2010; 20: 156–165.
- [9] Marco-Pallarés J, Münte TF, Rodríguez-Fornells A. The role of high-frequency oscillatory activity in reward processing and learning. *Neuroscience and Biobehavioral Reviews*. 2015; 49: 1–7.
- [10] Ahmadi A, Khorasani A, Shalchyan V, Daliri MR. State-based decoding of force signals from multi-channel local field potentials. *IEEE Access*. 2020; 8: 159089–159099.
- [11] Zhuang J, Truccolo W, Vargas-Irwin C, Donoghue JP. Decoding 3-D reach and grasp kinematics from high-frequency local field potentials in primate primary motor cortex. *IEEE Transactions on Bio-medical Engineering*. 2010; 57: 1774–1784.
- [12] Bundy DT, Pahwa M, Szrama N, Leuthardt EC. Decoding three-dimensional reaching movements using electrocorticographic signals in humans. *Journal of Neural Engineering*. 2016; 13: 026021.
- [13] Churchland MM, Cunningham JP, Kaufman MT, Foster JD, Nuyujukian P, Ryu SI, *et al*. Neural population dynamics during reaching. *Nature*. 2012; 487: 51–56.
- [14] Biro D, Freeman R, Meade J, Roberts S, Guilford T. Pigeons combine compass and landmark guidance in familiar route navigation. *Proceedings of the National Academy of Sciences of the United States of America*. 2007; 104: 7471–7476.
- [15] Zhao K, Wan H, Shang Z, Liu X, Liu L. Intracortical microstimulation parameters modulate flight behavior in pigeon. *Journal of Integrative Neuroscience*. 2019; 18: 23–32.
- [16] Cai L, Dai Z, Wang W, Wang H, Tang Y. Modulating motor behaviors by electrical stimulation of specific nuclei in pigeons. *Journal of Bionic Engineering*. 2015; 12: 555–564.
- [17] Cheng S, Li M, Yu H, Zhao K, Liu S, Wan H. Decoding Pigeon Behavior Outcomes during Goal-directed Decision Task by WSR Functional Network Analysis. *Annual International Conference of the IEEE Engineering in Medicine and Biology Society. IEEE Engineering in Medicine and Biology Society. Annual International Conference*. 2020; 2020: 38–41.
- [18] Massot B, Arthaud S, Barrillot B, Roux J, Ungurean G, Luppi PH, *et al*. ONEIROS, a new miniature standalone device for recording sleep electrophysiology, physiology, temperatures and behavior in the lab and field. *Journal of Neuroscience Methods*. 2019; 316: 103–116.
- [19] Wang L, Yang L, Li M, Yang Z, Shang Z. Development of wearable miniature neural signal recording system for birds. *2020 Chinese Automation Congress. Shanghai, 06-08 November 2020. IEEE: Washington*. 2020; 3493–3496.
- [20] Shang Z, Liang Y, Li M, Zhao K, Yang L, Wan H. Sequential neural information processing in nidopallium caudolaterale of pigeons during the acquisition process of operant conditioning. *Neuroreport*. 2019; 30: 966–973.
- [21] Karten H J, Hodos W. A stereotaxic atlas of the brain of the pigeon (*Columba livia*). Johns Hopkins Press: Baltimore. 1967.
- [22] Rehman Nu, Aftab H. Multivariate variational mode decomposition. *IEEE Transactions on Signal Processing*. 2019; 67: 6039–6052.
- [23] Taylor LA, Portugal SJ, Biro D. Homing pigeons (*Columba livia*) modulate wingbeat characteristics as a function of route familiarity. *The Journal of Experimental Biology*. 2017; 220: 2908–2915.
- [24] Usherwood JR, Stavrou M, Lowe JC, Roskill K, Wilson AM. Flying in a flock comes at a cost in pigeons. *Nature*. 2011; 474: 494–497.
- [25] Dell’Ariccia G, Dell’Omo G, Wolfer DP, Lipp HP. Flock flying improves pigeons’ homing: GPS track analysis of individual flyers versus small groups. *Animal Behaviour*. 2008; 76:1165–1172.
- [26] Kano F, Walker J, Sasaki T, Biro D. Head-mounted sensors reveal visual attention of free-flying homing pigeons. *The Journal of Experimental Biology*. 2018; 221: jeb183475.
- [27] Rubinov M, Sporns O. Complex network measures of brain connectivity: uses and interpretations. *NeuroImage*. 2010; 52: 1059–1069.
- [28] Xu J. An extended one-versus-rest support vector machine for multi-label classification. *Neurocomputing*. 2011; 74: 3114–3124.
- [29] Fell J, Axmacher N. The role of phase synchronization in memory processes. *Nature Reviews. Neuroscience*. 2011; 12: 105–118.
- [30] Canolty RT, Knight RT. The functional role of cross-frequency coupling. *Trends in Cognitive Sciences*. 2010; 14: 506–515.
- [31] Womelsdorf T, Valiante TA, Sahin NT, Miller KJ, Tiesinga P. Dynamic circuit motifs underlying rhythmic gain control, gating and integration. *Nature Neuroscience*. 2014; 17: 1031–1039.
- [32] Wang H, Li J, Cai L, Wang C, Shi A. Flight control of robo-pigeon using a neural stimulation algorithm. *Journal of Integrative Neuroscience*. 2018; 17: 337–342.
- [33] Fang K, Mei H, Tang Y, Wang W, Wang H, Wang Z, *et al*. Grade-control outdoor turning flight of robo-pigeon with quantitative stimulus parameters. *Frontiers in Neurorobotics*. 2023; 17: 1143601.
- [34] Wang H, Wu J, Fang K, Cai L, Wang LS, Dai ZD. Application of robo-pigeon in ethological studies of bird flocks. *Journal of Integrative Neuroscience*. 2020; 19: 443–448.
- [35] Mehlhorn J, Haastert B, Rehkämper G. Asymmetry of different brain structures in homing pigeons with and without navigational experience. *The Journal of Experimental Biology*. 2010; 213: 2219–2224.
- [36] Pollonara E, Guilford T, Rossi M, Bingman VP, Gagliardo A. Right hemisphere advantage in the development of route fidelity in homing pigeons. *Animal Behaviour*. 2017; 123: 395–409.
- [37] Biro D, Meade J, Guilford T. Familiar route loyalty implies visual pilotage in the homing pigeon. *Proceedings of the National Academy of Sciences of the United States of America*. 2004; 101: 17440–17443.